Crystal Construction and Molecular Recognition for $[Cr(CO)_6]$†

Dario Braga,[*,a] **Fabrizia Grepioni,**[a] **Emilio Tedesco**[a] **and A. Guy Orpen**[b]
[a] *Dipartimento di Chimica G. Ciamician, Università di Bologna, Via Selmi 2, 40126 Bologna, Italy*
[b] *School of Chemistry, University of Bristol, Bristol BS8 1TS, UK*

The molecular organization in crystals of the prototypical organometallic molecule $[Cr(CO)_6]$ has been investigated by means of packing-potential-energy calculations and computer graphics analysis. The atom–atom pairwise-potential-energy method has been used to study the interaction energy between molecular pairs and the molecular self-recognition process which leads to crystal construction. Alternative crystal structures have been generated and compared with the experimentally observed structure in terms of packing cohesion.

The possibility of generating hypothetical crystal structures from known molecular structures has always been an attractive task.[1] Previous work has been carried out in solid-state organic chemistry with remarkable achievements.[2] The study of the packing modes of aromatic hydrocarbons[3] and of the anomalous crystal-structure organization of adipamide[4] are two examples worth mentioning. More recently, this type of approach has been further developed by Gavezzotti[5] to generate crystal structures for low-polarity organic compounds.[5]

We have recently reported the results of a crystal-generation study carried out on $[Ni(CO)_4]$ and $[Fe(CO)_5]$.[6] These two molecules were chosen because they possess prototypical molecular shapes, *viz.* the tetrahedron and the trigonal bipyramid, respectively thus constituting a representative sample for the investigation of the intermolecular self-recognition and interlocking in neutral organometallic systems. We were able to find several hypothetical crystal structures which could be compared with the experimentally determined ones in terms of efficiency of packing and of cohesion. Among these the observed crystal structures could be retraced. We were also able to calculate theoretical packing arrangements for the hypothetical square-pyramidal isomer of the $[Fe(CO)_5]$ molecule.

We now report on the extension of this study to the molecular and crystal structure of $[Cr(CO)_6]$. This molecule, with its regular octahedral co-ordination geometry, represents the prototype of octahedral complexes.[7] The compounds $[Mo(CO)_6]$, $[W(CO)_6]$ and the seventeen-electron species $[V(CO)_6]$ are all isostructural with $[Cr(CO)_6]$.[8] The main features of the solid-state structure of $[Cr(CO)_6]$ as obtained from the original structural work can be briefly summarized as follows. (*i*) The crystalline complex has been subjected to both X-ray[7a] and neutron diffraction[7b] studies carried out at room temperature and at 78 K, respectively. (*ii*) It crystallizes in the orthorhombic space group *Pnma* with $Z = 4$. The molecule is bisected by a crystallographic mirror plane which comprises two *trans* ligands [C(1)O(1), C(2)O(2)] and the Cr atom; two carbonyls are in general positions and related to the remaining two by the mirror plane. (*iii*) The Cr–C and C–O distances of the six carbonyls are equivalent within standard deviations. (*iv*) As do all other binary carbonyls, $[Cr(CO)_6]$ forms a typical molecular crystal in which the molecules are held together by van der Waals interactions according to the same close-packing principles as apply for organic substances.[9] Each molecule in the crystal is surrounded by twelve first neighbours distributed in anticuboctahedral fashion.

This paper is organized in two main sections. In the first the atom–atom pairwise-potential-energy method is applied to decode the experimentally determined crystal structure. Attention is focused on the most efficient intermolecular interactions between the reference molecule and the first neighbouring ones. In the second section dimolecular nuclei are constructed starting from the molecular structure of $[Cr(CO)_6]$. These are compared in terms of cohesive energy with the experimental ones and are then used to generate three-dimensional arrays by translational symmetry. The calculated crystal structures are then compared with the experimental one. The reader is addressed to ref. 5 for details of the application of these methods to organic molecules; refs. 6 and 9(*b*) discuss previous applications to organometallic systems.

Crystal Structure Decoding

According to the atom–atom pairwise-potential-energy method[10] it is possible to calculate, starting from the knowledge of the crystal structure, an approximate value of the packing potential energy (p.p.e.).[11] The packing coefficient (p.c.) can also be estimated according to the formula p.c. = $V_{mol}Z/V_{cell}$ where V_{mol} is calculated[12] with the method of the 'intersecting cups' of Kitaigorodsky.[10a]

Since the potential parameters are calibrated on crystal structures determined at room temperature, we will confine our analysis of the experimental structure to the X-ray determined crystal structure. The neutron structure at 78 K can be used to see the effect of the temperature decrease on the volume occupation in the lattice. As expected, the difference in temperature is reflected in the difference in packing coefficients which increases from 0.68 to 0.73 on going from room temperature to 78 K.

The p.p.e. was calculated with the generalized potential parameters obtained by Gavezzotti and Filippini[13a] for the C and O atoms, while the Cr atom was treated, as usual, as the corresponding noble gas, krypton. At room temperature a value of -38.7 kcal mol^{-1} was obtained. This value is more cohesive than that reported previously[9a] (-31.2 kcal mol^{-1}) obtained by using the alternative set of potential parameters for the light atoms put forward by Mirsky.[13b]

The room-temperature experimental structure was used as starting point in the structural relaxation stage. This procedure is necessary to test the effect of the parameter choice on the

---

† *Non-SI unit employed:* cal = 4.184 J.

structure under investigation. A good choice of potential parameters (to be used subsequently for crystal construction) is expected to produce only small displacements from the observed structures. The generalized potential parameters mentioned above were found to be best suited at this stage in agreement with our previous tests in the cases of [$Ni(CO)_4$] and [$Fe(CO)_5$]. A list of atom–atom potential parameters is provided in Table 1.

As it can be seen from Table 2, crystal-structure relaxation leaves the starting room-temperature structure essentially unchanged. Crystal relaxation was performed using PCK 83.[14] Space- and point-group symmetry were preserved in the calculations, *viz.* cell axes were refined, but not the cell angles; analogously, molecular rotation and translation were constrained to occur with *m* symmetry preserved. The total rigid-body translation (ΔX) and rotational displacements ($\Delta\chi$) after crystal-structure relaxation were small, $\Delta X = 0.088$ Å and $\Delta\chi = 0.46°$, respectively.

We first seek the most cohesive dimolecular nuclei present in the observed structure, *viz.* the experimental structure is (rather artificially) 'partitioned' in its most relevant contribution to the total p.p.e. The molecules surrounding the one chosen for reference are listed in Table 3 together with the individual contribution to the p.p.e. and the symmetry operations that generate them. From this table the most cohesive interlocking motifs are clearly identified, and can be compared with those obtained theoretically in the dimer search described below.

In the experimental structure the 'best' dimolecular nuclei are generated by a screw axis [see Fig. 1(*a*)]. The interlocking is such that one CO of one molecule interacts with a trigonal unit formed by two equatorial and one axial CO of the neighbouring molecule. The interaction energy (cohesive energy, c.e.) is −3.7 kcal mol^{-1} and the intermolecular separation between the Cr atoms is 6.339 Å.

The second most cohesive dimolecular nuclei are obtained by pure translation (along the unit cell *z* axis, symmetry operations 3 and 4 in Table 3); its c.e. is −3.6 kcal mol^{-1}. The intermolecular separation is slightly shorter (6.332 *vs.* 6.339 Å). The interlocking is simple to describe: one axial CO is embraced by two equatorial CO groups of a neighbouring molecule, as shown in Fig. 1(*b*). A space-filling representation of the experimental structure is shown in Fig. 2.

Table 1 Parameters for the packing potentials. The p.p.e. calculations and crystal-structure refinement was carried out by using the Buckingham-type potential function $Ae^{-Br} - Cr^{-6}$ (kcal mol^{-1}; *r* in Å). Cross-interactions were calculated from $A_{xy} = A_{xx}^{\frac{1}{2}}A_{yy}$, $B_{xy} = \frac{1}{2}(B_{xx} + B_{yy})$, $C_{xy} = C_{xx}^{\frac{1}{2}}C_{yy}$

Kr···Kr	270 600	3.28	3 628
Mirsky[13b]	*A*	*B*	*C*
C···C	71 600	3.68	421
O···O	77 700	4.18	259.4
H···H	4 900	4.29	29
C···H	18 600	3.94	118
C···O	75 700	3.91	339.4
O···H	19 500	4.23	88
Gavezzotti and Filippini[13a]			
C···C	54 050	3.47	578
O···O	46 680	3.74	319
H···H	4 900	4.29	29
C···H	16 274	3.88	129
C···O	93 950	3.74	641
O···H	15 124	4.01	96

Table 2 Structure relaxation on the experimental crystal structure

	Space group *Pnma* treated in $P2_12_12_1$	
	Exptl.*	Relaxed
a/Å	11.769	11.652
b/Å	11.092	11.031
c/Å	6.332	6.272
U/Å^3	826.59	806.16
p.c.	0.68	0.69
p.p.e. kcal mol^{-1}	−38.7	−39.1

* Crystal structure at room temperature.

Packing Generation, Calculation of Dimolecular Nuclei

The construction of dimolecular nuclei is the initial step of the crystal-generation procedure. The nuclei obtained *via* **PROMET**[15] will now be briefly described. The most common symmetry operators (the translation **T**, the screw axis **S**, and the centre of inversion **I**) are applied in the space surrounding the reference molecule. The most cohesive dimolecular nuclei are selected on the basis of the interaction energy between the two symmetry-related molecules forming them. The energy of the dimer is obtained by means of the same potential function described above. It is important to appreciate that the construction of the dimolecular nuclei is not only the first step in the crystal-generation procedure, but also the point at which unsatisfactory nuclei, and therefore crystals, are sifted out.

Once the dimolecular nuclei are chosen, translation in the three directions of space is applied to generate calculated crystal structures which are then optimized as in the case of the experimental structure (see above). The space groups obtained by combining the **I**- and **S**-dimolecular nuclei with the **T**, **I** and **S** operators are shown in Table 4.

At this stage, one may wonder why we have chosen to study [$Cr(CO)_6$] since it does not crystallize in any of the space groups listed in Table 5. Moreover the experimental space group *Pnma* is found in only 2.4% of the crystal structures of organometallic molecules characterized to date according to our previous search[6] of space-group frequencies in the Cambridge Data Base. It is important to appreciate, however, that higher-symmetry space groups can be generated by convolution of molecular symmetry and crystal symmetry. Given the high molecular symmetry of [$Cr(CO)_6$] the crystal-

Table 3 Symmetry operations and individual contribution to the p.p.e. of the molecules forming the first neighbouring shell in the experimental crystal structure of [$Cr(CO)_6$]

Number	Symmetry operation	p.p.e. contribution/ kcal mol^{-1}
1	$x + \frac{1}{2}, -y + \frac{1}{2}, -z + \frac{1}{2}$	−3.7
2	$x - \frac{1}{2}, -y + \frac{1}{2}, -z + \frac{1}{2}$	−3.7
3	$x, y, z - 1$	−3.6
4	$x, y, z + 1$	−3.6
5	$-x, y - \frac{1}{2}, -z$	−3.5
6	$-x, y + \frac{1}{2}, -z$	−3.5
7	$x - \frac{1}{2}, -y + \frac{1}{2}, z - \frac{1}{2}$	−2.2
8	$-x + \frac{1}{2}, -y, z - \frac{1}{2}$	−2.2
9	$x + \frac{1}{2}, -y + \frac{1}{2}, -z - \frac{1}{2}$	−2.2
10	$-x + \frac{1}{2}, -y, z + \frac{1}{2}$	−2.2
11	$-x + \frac{1}{2}, -y + 1, z - \frac{1}{2}$	−2.2
12	$-x + \frac{1}{2}, -y + 1, z + \frac{1}{2}$	−2.2

Table 4 Space groups resulting from combination of **T**, **I** and **S** operators

Initial dimolecular nuclei	Symmetry operator	Space group
T	**T**	$P1$
I	**I**+**T**	$P\bar{1}$
S	**S**+**T**	$P2_1$
S	**S**+**I**+**T**	$P2_1/c$
I	**I**+**S**+**T**	$P2_1/c$
S	**S**+**S**+**T**	$P2_12_12_1$

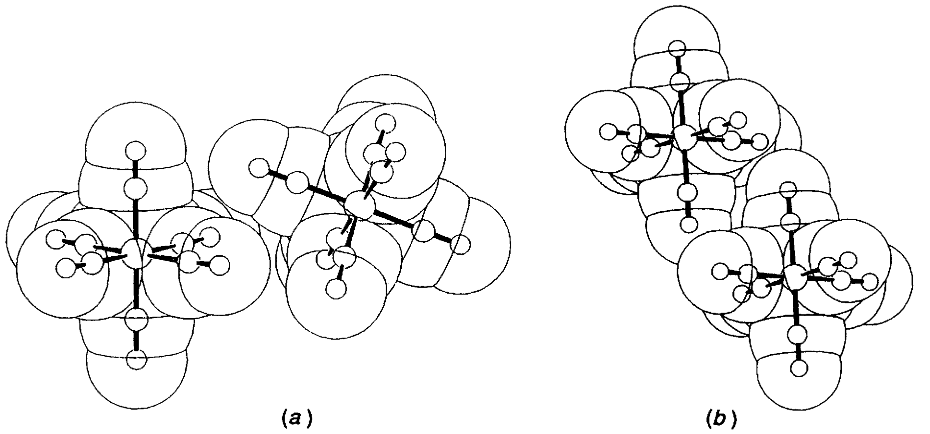

(a) (b)

Fig. 1 Decoding the experimental crystal structure. (*a*) The 'dimer' formed by two $[Cr(CO)_6]$ molecules interlocked along the screw-fold axis; the two Cr atoms are 6.339 Å apart at room temperature, one CO of one molecule interacts with a trigonal unit formed by two equatorial and one axial CO of the neighbouring molecule. (*b*) The interlocking motif along the *z* axis; the two Cr atoms are 6.332 Å apart, and one axial CO is embraced by two equatorial carbonyls of the neighbouring molecule

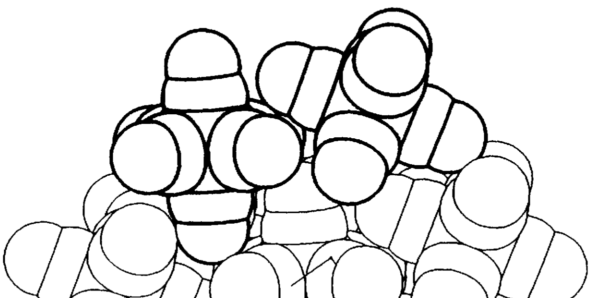

Fig. 2 Space-filling representation of the experimental structure; thick lines show the S-dimolecular nuclei

structure search will necessarily lead to optimized structures in space groups which are subgroups of those attainable if such molecular and crystal symmetry convolution is taken into account.

The results of the dimolecular nuclei search and subsequent crystal-structure generation are summarized in Table 5 together with alternative unit-cell settings. Only the most representative (*i.e.* most cohesive) solutions are reported and compared with the experimental one. The most cohesive nuclei in each calculated crystal structure are also reported.

*Triclinic P*1.—A triclinic *P*1 crystal can be obtained by applying only translational symmetry in the three directions of space. Solution Cr-TA in Table 5 appears to be competitive with Cr-OBS. The translational dimolecular nuclei along the *x* axis [Fig. 3(*a*)] is very similar to that present experimentally [compare Figs. 3(*a*) and 1(*b*)]. The Cr $\cdots$ Cr separation (6.122 Å) is slightly smaller than the experimental one, and the resulting crystal possesses comparable density and energy cohesion (p.c. 0.70 *versus* 0.68, p.p.e. -38.6 *versus* -37.72 kcal mol^{-1}). A space-filling representation of structure Cr-TA is shown in Fig. 3(*b*).

Triclinic P$\bar{1}$.—As expected on the basis of the high molecular symmetry of $[Cr(CO)_6]$, the inversion centre generates **I**-dimolecular nuclei which are very similar to that obtained by pure translation with an interaction energy of -3.8 kcal mol^{-1} and an intermolecular separation of 6.227 Å [compare Fig. 4 with 1(*b*) and 3(*a*)]. The triclinic and centrosymmetric structure (Cr-I2 in Table 5) obtained is comparable in p.p.e. and p.c. with the experimental one.

Monoclinic P2_1.—In the calculated S-dimolecular nuclei, one axial CO of one molecule points towards a trigonal unit of a neighbouring one as shown in Fig. 5. This interlocking motif is less efficient than other calculated ones, and results in a Cr $\cdots$ Cr separation of 7.08 Å, with c.e. = -2.3 kcal mol^{-1}. In fact the most cohesive dimolecular nuclei in the $P2_1$ structure Cr-S1 are not those generated by the S-nucleus search but those obtained *via* translational symmetry ($\mathbf{T}_y$, Cr $\cdots$ Cr 5.931 Å, c.e. = -4.8 kcal mol^{-1}). This apparently contradictory result is of some relevance because it demonstrates that the initial stage, *i.e.* the dimolecular nuclei generation procedure, does not bias the subsequent three-dimensional search. Therefore the final most cohesive molecule–molecule interaction is not *necessarily* that of the input dimolecular nuclei. The $P2_1$ structure is reminiscent of that observed, the two principal interactions being those obtained *via* the S- and **T** operators. The cell parameters and the angles [which are all close to 90° in spite of the monoclinic (and not orthorhombic) constraints on the search] are similar to the experimental ones. There is, in fact, a fairly simple relationship between the unit cell axes of the experimental structure and those of solution Cr-S1: the *c* and *b* axes in the former coincide with *a* and *c* in the latter structure, whereas the *a* axis in the experimental structure is almost double that of the *b* axis in Cr-S1 (see the alternative unit-cell setting in Table 5).

Monoclinic P$2_1/c$.—The subsequent application of an inversion centre to preconstructed S-dimolecular nuclei (the same as generated from the S search in space group $P2_1$) yields a crystal structure in space group $P2_1/c$. Solution Cr-S11, however, does not seem to represent an alternative or competitive structure with respect to those obtained in lower-symmetry space groups and discussed above. Although the molecules in the final dimolecular nuclei are closely interlocked (Cr $\cdots$ Cr 5.778 Å, the shortest attained) the overall structure is poorly cohesive.

Orthorhombic P$2_12_12_1$.—The structural search in space group $P2_12_12_1$ is more informative. Crystals can be obtained by applying the S search on preconstructed S-dimolecular nuclei.

Table 5 Crystal data and dimolecular nuclei calculated and observed structures

Code	Space group	Symmetry operator	Dimolecular nuclei Cr $\cdots$ Cr/Å	c.e./ kcal mol^{-1}	p.p.e./ kcal mol^{-1}	p.c.	a^*/Å	b^*/Å	c^*/Å	U/Å^3	α^*/°	β^*/°	γ^*/°
Cr-OBS	*Pnma* treated in $P2_12_12_1$	**S**	6.339	−3.7	−38.72	0.68	11.769	11.092	6.332	826.6	90.0	90.0	90.0
		$\mathbf{T}_z$	6.332	−3.4									
Cr-TA	$P1$	$\mathbf{T}_x$	6.122	−3.6	−38.6	0.70	6.122 (6.237)	6.237 (7.000)	7.030 (6.122)	202.0	63.41 (15.8)	90.51 (18.6)	61.4 (63.9)
Cr-I2	$P\bar{1}$	**I**	6.227	−3.8	−38.6	0.69	6.244 (6.319)	6.319 (10.845)	15.441 (6.244)	409.8	116.9 (104.3)	50.5 (98.1)	98.1 (91.2)
Cr-S1	$P2_1$	$\mathbf{T}_y$	5.931	−4.8	−37.8	0.68	6.332 (6.332)	5.931 (11.033)	11.033 (5.931)	414.3	90.0 (90.0)	89.3 (90.0)	90.0 (90.0)
		S	7.080	−2.3									
Cr-S1I	$P2_1/c$	**S**	5.778	−5.1	−33.1	0.63	6.234 (11.555)	12.555 (12.555)	16.913 (6.234)	904.3	90.0 (90.0)	43.1 (90.0)	90.0 (90.0)
		I	6.381	−3.6									
Cr-S1S	$P2_12_12_1$	$\mathbf{T}_y$	6.142	−3.9	−37.7	0.68	11.119 (11.119)	6.142 (12.187)	12.187 (6.142)	832.3	90.0 (90.0)	90.0 (90.0)	90.0 (90.0)
		S	6.359	−3.5									
		S	6.805	−2.7									

* Values for Niggli reduced cells and alternative unit cell settings are in parentheses.

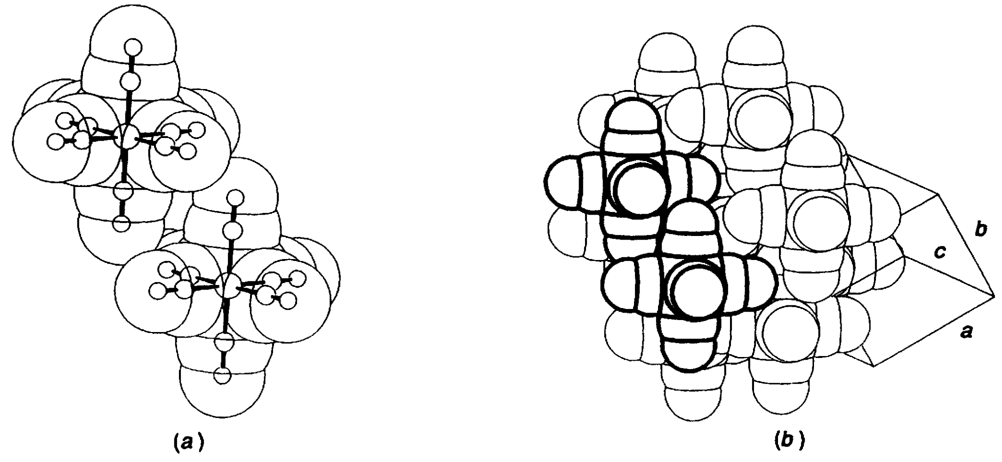

Fig. 3 (a) Dimolecular nuclei calculated for a triclinic $P1$ crystal, compare with the T_z-nuclei present in the experimental crystal structure of $[Cr(CO)_6]$. (b) Space-filling representation of the solution Cr-TA; thick lines show the dimolecular nuclei

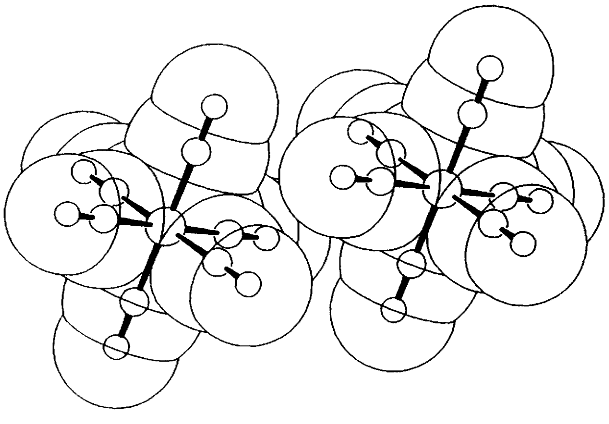

Fig. 4 The I-dimolecular nuclei present in the calculated $P\bar{1}$ structure Cr-I2; compare with Fig. 3(a)

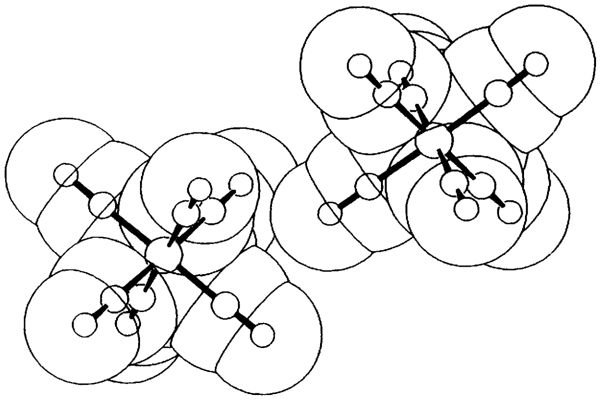

Fig. 5 The most cohesive S-dimolecular nuclei in the calculated $P2_1$ crystal

Solution Cr-S1S presents some interesting features. A space-filling representation is shown in Fig. 6. The most cohesive dimolecular nuclei (-3.9 kcal mol^{-1}) is generated by pure translation along the *b* axis, whereas those generated by the S operators are less cohesive contributing -3.5 and -2.7 kcal mol^{-1}, respectively (see Table 5). The latter S-dimolecular nuclei (shown in Fig. 6) are similar in terms of relative orientation of the constituent molecules to the S-dimolecular nuclei present experimentally. Although the energy ranking of the T- and S-dimolecular nuclei is different, solution Cr-S1S presents p.p.e. and p.c. values which are comparable to the experimental ones.

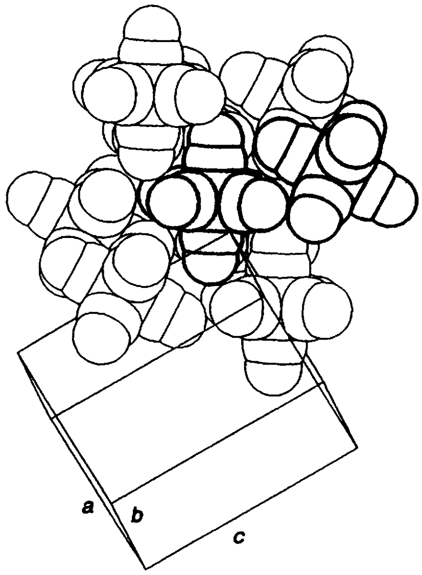

Fig. 6 A space-filling representation of solution Cr-S1S; compare with Fig. 2

From a comparison of Fig. 6 and 2 and from the values reported in Table 5, it can be appreciated that solution Cr-S1S and the experimental structure are closely similar albeit with different axis labels. Hence, the crystal-structure generation procedure has successfully retraced the observed crystal structure of $[Cr(CO)_6]$

Conclusion

In this paper we have attempted the generation of theoretical crystal structures for the prototypical octahedral complex $[Cr(CO)_6]$ starting from its molecular structure. Our approach has been the same as that previously developed and tested on $[Ni(CO)_4]$ and $[Fe(CO)_5]$. Beside yielding alternative crystal structures, it also allows one to explore how two molecules of $[Cr(CO)_6]$ can interact and interlock. The problem is that of the relationship between the structure of one molecule and the structure of an ordered three-dimensional collection of such molecules.

We have been able to show that efficient interlocking of octahedral molecules can be achieved *via* translational symmetry (or higher symmetry operators if the convolution of molecular with crystal symmetry is considered) and *via* the screw axis. The calculated dimolecular nuclei have been used in the subsequent three-dimensional search to generate new crystal structures. The results have been compared, in terms of cohesive energy and of efficiency molecular packing, with the experimentally observed structure. The latter has been retraced in the correct symmetry subgroup of the original *Pnma* space group. This is of some importance since it demonstrates that even in the cases of highly symmetrical molecules the observed intermolecular arrangements can be attained by treating the whole molecular entity in a lower-symmetry space group.

It is interesting that, apart from the $P2_1/c$ crystal, all other solutions are within 1 kcal mol^{-1} of the experimental one. The implication is two-fold: on one hand it may suggest that the potential parameters employed in the search procedure have limited discriminatory power {we have met with the same problem in our previous study of $[Ni(CO)_4]$ and $[Fe(CO)_5]$}, on the other hand, however, it may suggest the possible existence of polymorphic forms of even a geometrically simple molecule such as $[Cr(CO)_6]$. Polymorphic modifications are known for other octahedral molecules such as SF_6 (observed in space groups $I\bar{4}3m$, $P\bar{1}$, $C2/m$ and $Im\bar{3}m$)[16] as well as for MoF_6 which crystallizes both in *Pnma*, *viz.* isomorphous with $[Cr(CO)_6]$, and in *I*432.[17] Crystals of space group *Pnma* are also formed by TeF_6,[18] UF_6[19] and WF_6.[20] In all these cases molecular symmetry is convoluted with space-group symmetry.

We believe that the method outlined in this paper for the organometallic solid state can have useful applications such as, for example, the *ab-initio* proposition of crystal structure(s) starting from molecular structures of neutral organometallic molecules, determined theoretically or by methods alternative to diffraction.

Acknowledgements

It is a pleasure to thank Professor Angelo Gavezzotti for many useful discussions and for continuous help and encouragement. D. B. and F. G. acknowledge Consiglio Nazionale delle Ricerche for financial support, A. G. O. the Ciba-Geigy Foundation for the award of a Senior Research Fellowship.

References

1 J. Maddox, *Nature (London)*, 1988, **335**, 201; J. Perlstein, *J. Am. Chem. Soc.*, 1994, **116**, 455.
2 P. Dauber and A. T. Hagler, *Acc. Chem. Res.*, 1980, **13**, 105.
3 J. Bernstein, J. A. R. P. Sarma and A. Gavezzotti, *Chem. Phys. Lett.*, 1990, **174**, 361.
4 A. T. Hagler and L. Leiserowitz, *J. Am. Chem. Soc.*, 1978, **78**, 5879; L. Leiserowitz and A. T. Hagler, *Proc. R. Soc. London, Ser. A*, 1983, **388**, 133.
5 A. Gavezzotti, *J. Am. Chem. Soc.*, 1991, **113**, 4622.
6 D. Braga, F. Grepioni and A. G. Orpen, *Organometallics*, 1994, **13**, 3544.
7 (*a*) A. Whitaker and J. W. Jeffery, *Acta Crystallogr.*, 1967, **23**, 977; (*b*) B. Rees and A. Mitschler, *J. Am. Chem. Soc.*, 1978, **98**, 7918.
8 S. P. Arnesen and H. M. Seip, *Acta Chem. Scand.*, 1966, **20**, 2711; S. Bellard, K. A. Rubinson and G. M. Sheldrick, *Acta Crystallogr. Sect. B*, 1979, **35**, 271.
9 (*a*) D. Braga, F. Grepioni and P. Sabatino, *J. Chem. Soc., Dalton Trans.*, 1990, 3137; (*b*) D. Braga, F. Grepioni, P. Sabatino and A. Gavezzotti, *J. Chem. Soc., Dalton Trans.*, 1992, 1185.
10 (*a*) A. I. Kitaigorodsky, *Molecular Crystal and Molecules*, Academic Press, New York, 1973; (*b*) A. J. Pertsin and A. I. Kitaigorodsky, *The Atom–Atom Potential Method*, Springer, Berlin, 1987.
11 A. Gavezzotti and M. Simonetta, *Chem. Rev.*, 1981, **82**, 1.
12 A. Gavezzotti, *J. Am. Chem. Soc.*, 1989, **111**, 1835.
13 (a) A. Gavezzotti and G. Filippini, *Acta Crystallogr., Sect. B*, 1993, **49**, 868; (*b*) K. Mirsky, *Computing in Crystallography, Proceedings of the International Summer School on Crystallographic Computing*, Delft University Press, Twente, 1978, p. 169.
14 D. E. Williams, PCK 83, A Crystal Molecular Packing Analysis Program, Quantum Chemistry Program Exchange no. 481, Indiana University, Bloomington, IN.
15 A. Gavezzotti, **PROMET**, A Program for the Generation of Possible Crystal Structures from the Molecular Structure of Organic Compounds, Mark version I, Milano, 1993.
16 D. Bellamy, D. Braga, F. Grepioni and A. G. Orpen, unpublished work.
17 J. C. Taylor and A. B. Waugh, *J. Solid State Chem.*, 1976, **18**, 241; B. M. Powell, M. T. Dove, G. S. Pawley and L. S. Bartell, *Mol. Phys.*, 1987, **62**, 1127; J. K. Cockcroft and A. N. Fitch, *Z. Kristallogr.*, 1988, **184**, 123.
18 J. H. Levy, J. C. Taylor and P. W. Wilson, *Acta Crystallogr., Sect. B*, 1975, **31**, 398; J. H. Levy, J. C. Taylor and A. B. Waugh, *J. Fluorine Chem.*, 1983, **23**, 29; H. J. Levy, P. L. Sanger, J. C. Taylor and P. W. Wilson, *Acta Crystallogr., Sect. B*, 1975, **31**, 1065.
19 L. S. Bartell and B. M. Powell, *Mol. Phys.*, 1992, **75**, 689.
20 J. H. Levy, J. C. Taylor and P. W. Wilson, *J. Chem. Soc., Dalton Trans.*, 1976, 219; J. C. Taylor, P. W. Wilson and J. W. Kelly, *Acta Crystallogr., Sect. B*, 1973, **29**, 7; J. C. Taylor and P. W. Wilson, *J. Solid State Chem.*, 1975, **14**, 378.
21 J. H. Levy, J. C. Taylor and P. W. Wilson, *J. Solid State Chem.*, 1975, **15**, 360.

Received 1*st September* 1994; *Paper* 4/05331A